amse
école d'économie d'aix-marseille
aix-marseille school of economics

Working Papers / Documents de travail

The Dynamic Effects of Weather Shocks on Agricultural Production

Cédric Crofils
Ewen Gallic
Gauthier Vermandel

WP 2024 - Nr 02

The Dynamic Effects of Weather Shocks on Agricultural Production †

Cédric Crofils✉[a,b], Ewen Gallic[b], and Gauthier Vermandel[c,d,a]

[a]LEDa, Paris-Dauphine & PSL Universities
[b]Aix Marseille Univ, CNRS, AMSE, Marseille, France.
[c]CMAP, Ecole polytechnique, Institut Polytechnique de Paris
[d]Banque de France, 31 rue Croix des Petits Champs, 75049 Paris, France.

February 2, 2024

Abstract

This paper investigates the dynamic effects of weather shocks on monthly agricultural production in Peru, using a Local Projection framework. An adverse weather shock, measured by an excess of heat or rain, always generates a delayed negative downturn in agricultural production, but its magnitude and duration depend on several factors, such as the type of crop concerned or the timing at which it occurs. On average, a weather shock –a temperature shock– can cause a monthly decline of 5% in agricultural production for up to four consecutive months. The response is time-dependent: shocks occurring during the growing season exhibit a much larger response. At the macroeconomic level, weather shocks are recessionary and entail a decline in inflation, agricultural production, exports, exchange rate and GDP.

JEL classification Numbers: C23, E32, Q11, and Q54

Keywords: Weather shocks, Agriculture, Local projections, VAR

†We thank Olivier Deschenes, Garance Genicot, Loïc Henry, Elise Huillery, Evi Pappa, Aymeric Ortmans, Emilien Veron and Juan-Pablo Rud for their remarks, as well as seminar participants at University College London, Université Paris-Dauphine. We also thank the contributors at the conferences where this research was presented: the EEA Congress 2023, the EAERE 28th Annual Conference, the 29th CEF International Conference, The AFSE 2023 Annual Congress, the 22nd Journées LAGV, the 20th Augustin Cournot Doctoral Days, the 12th EconomiX PhD Student Conference, the Dauphine Economics Doctoral Day, the 95th International Atlantic Economic Conference, Banque de France Clifirium conference, and Stress-test seminar of Institut Polytechnique for their valuable and insightful feedback.
Cedric Crofils acknowledges funding from the Collectivité Territoriale de Martinique. Ewen Gallic acknowledges that the project leading to this publication has received funding from the French government under the "France 2030" investment plan managed by the French National Research Agency (reference: ANR-17-EURE-0020) and from the Excellence Initiative of Aix-Marseille University – A*MIDEX. Gauthier Vermandel acknowledges funding from the chair Stress-test hosted by Institut Polytechnique de Paris.

✉Corresponding author: cedric.crofils@dauphine.psl.eu. University Paris Dauphine – PSL Research University, LEDa UMR CNRS 8007, Place du Maréchal de Lattre de Tassigny, 75775 Paris Cedex 16, France.

1 Introduction

Of all economic sectors, agriculture stands out as the most vulnerable to weather fluctuations. In developing countries, the agricultural sector is a major contributor to aggregate production, in terms of output and employment. In these economies, abnormal weather realizations – or weather shocks – can have significant economic consequences (Mendelsohn, 2009). Because many small-scale farmers in developing countries have limited access to risk management tools such as insurance and irrigation infrastructure, these economies are also particularly vulnerable to exogenous shifts in weather conditions (Aragón et al., 2021). Consequently, weather shocks can have a disproportionate impact on livelihood and food security.

Given these vulnerabilities, the objective of this study is to quantitatively measure the dynamic effects of abnormal weather on the supply of agricultural products over time. Assessing the consequences of an unexpected weather event observed today on future crop production is essential for anticipating adverse outcomes. This is particularly crucial in the context of climate change, where certain countries, especially in the tropics, face significant increases in temperature and precipitation variability (Castellanos et al., 2022). At the farmer level, such a quantitative analysis can aid in making better-informed decisions to adapt to climate change. At the macroeconomic level, these assessments are important for policymakers to anticipate potential food shortages and income losses, enabling them to implement effective mitigation policies.

Our empirical approach examines the impact of weather fluctuations on agricultural production in Peru, using monthly regional and crop-specific data. The analysis employs a linear panel model with local projections to leverage exogenous within-regional variations in weather fluctuations to assess how random changes in the weather affect agricultural production across months, regions, and crops. Our measures of weather shocks are based on precipitation and temperature. We compute the average monthly maximum regional extreme daytime temperature and total rainfall and express each as a weather anomaly by taking the deviation of the variable from its historical average.[1] We study the effects of weather shocks on production rather than on yields. The literature has traditionally focused on yield rather than production. However, as indicated by Iizumi and Ramankutty (2015), when calculating agricultural yields, all information regarding the quantity produced and available is lost. Indeed, in the event of a weather disruption to crop growth, farmers may choose to abandon a part of their production if the cost of harvesting outweighs the expected profit or if harvesting is no longer feasible. However, the yields observed at the end of the season do not reflect

[1] Intergovernmental Panel on Climate Change (IPCC) studies, such as Parry et al. (2007), have documented a large negative sensitivity of crop production to extreme daytime temperatures and precipitation. We build on this observation to construct the weather variables.

these decisions. This idea is reiterated by Lesk et al. (2016), who argue that the volume of production plays a role in determining food security, whereas yields do not.

The literature examining how the weather affects agricultural production typically bases its quantitative analysis on annual data (see, e.g., Jagnani et al., 2020; D'Agostino and Schlenker, 2016; Burke and Emerick, 2016; Deschênes and Greenstone, 2007). This widespread use of annual data poses two important limitations that can potentially underestimate the cost of weather shocks, and hence climate change. The first limitation concerns the *time-aggregation bias* of weather data. As weather data are typically provided at a higher frequency than economic data, their temporal aggregation is likely to omit relevant information (Cui et al., 2022) regarding their effects on agriculture. In particular, a standard mean-wise aggregation of extreme positive and negative events can be averaged out throughout the year (Colacito et al., 2019), thus underestimating the damages of the weather on agriculture. The second limitation concerns the role of the biological growing process of crops, which we refer here as the *crop growth bias*. Indeed, the growing process introduces a natural time lag between the realization of the weather shock and its economic materialization in terms of output loss at harvesting time. In addition, the vulnerability of crops varies depending on their growth stage, as crops are typically more vulnerable at the early stage than at the harvesting stage.

This article proposes two methodical contributions to avoid potential bias from weather time aggregation and crop growth process. First, to be immune to temporal aggregation effects, this study exploits the high-frequency nature of our agricultural production data. The original time dimension of our sample allows for a more precise mapping of economic costs and random weather variations without the information loss that occurs when averaging weather variables over a too long time span. The resulting risk of information loss emerging from the aggregation process is reduced. Second, to be immune to crop growth bias, this article employs local projections to track the effects of weather shocks along the growing process of crops. Local projections (LPs), pioneered by Jordà (2005), have become widely used econometric tools for measuring impulse response functions. LPs are not only relatively more robust to misspecification, but are also easy to estimate (via linear regression) and accommodate in panel data. We exploit the plausibly exogenous variations in temperature and precipitation at the Peruvian regional level to study the delayed effects of weather shocks on agricultural production over multiple periods after the realization of the shock. We control for fixed regional and macroeconomic characteristics. Then, by exploiting the cross-sectional dimension at the regional level, we use impulse response analysis to measure the propagation of a regional weather shock on agricultural production. Impulse response analysis is particularly well-suited for analyzing the cost of weather shocks disseminated over time through the natural growth process of crops.

Our main finding is that adverse weather shocks always result in a negative downturn in agricultural production. The extent and duration of this decline depend on various factors, such as the type of crops, type of weather shock, and season (growing season versus harvesting season). We find that a weather shock can cause a significant 5% monthly decline in agricultural production for up to four consecutive months for any crop type in the sample. Our second key finding emphasizes the role of crop growth timing in determining the response of agricultural production to weather fluctuations. Weather shocks that occur during the growing season have a more substantial impact than those occurring during the harvest season. Finally, our third principal takeaway is the response at the aggregate level. We find that a representative weather shock results in a 0.5% decline in agricultural GDP, a 1.5% decline in exports, and a modest reduction in inflation.

Our study is connected to two complementary branches of literature. The first strand of the literature examines the nexus between economic growth and climate based on yearly data. Dell et al. (2012) demonstrate that higher temperatures reduce economic growth and agricultural production in a large panel of countries. Building on this study, the research question has been extended in several directions.[2] Colacito et al. (2019) conduct a similar exercise for the US economy and find that rising summer temperatures have a pervasive effect on the entire cross-section of industries. Ortiz-Bobea et al. (2021) employ a country-level panel regression and yearly data from 1961 to 2015 to investigate the impact of climate change on agricultural Total Factor Productivity (TFP). The authors conclude that, on average, in Latin America, climate change had a negative impact on agricultural TFP, reducing it by more than 25% over the sample period, attributable to variations in average temperature and total rainfall.

The second strand of literature focuses on estimating the effects of weather and climate change on agriculture, employing agronomic models and statistical models (see D'Agostino and Schlenker 2016 for a review). The latter, which is predominant in the economic literature, has shifted from cross-sectional (Mendelsohn et al., 1994) to panel data analysis (see Blanc and Schlenker 2017, or Kolstad and Moore 2020). These models, which assess variables, such as crop yield (Schlenker and Roberts 2009), production (Lesk et al. 2016), and profit (Deschênes and Greenstone 2007) over space and time, account for both group- and time-specific effects. The former captures constants such as soil quality, while the latter considers factors affecting all regions in a given year. Panel regressions, treating weather variations as exogenous, offer insights into short-term effects, although caution is needed in long-term studies, as rapid farmer adaptation

[2]While most of the literature examines the effects of weather variables on quantities, Faccia et al. (2021) explore the effects on prices and identify deflationary effects.

can skew the results (Kolstad and Moore, 2020).[3] Our study relies on panel data such as this second strand of literature, and focuses on short-term effects. However, we adopt a distinct framework that not only links year-to-year variations in agricultural production with changing weather conditions but also facilitates the exploration of dynamic propagation effects.

This study makes three major contributions to the literature. First, the high frequency of our data enables the capture of infra-annual variations in production and their correlation with corresponding weather fluctuations. While most of the literature uses annual panel data and exploits year-to-year variations by aggregating the weather conditions over the growing season, our approach provides a finer mapping between the realization of the weather shock and its economic materialization.

Second, we employ the Local Projection method to examine the impact of weather fluctuations on production. Although this method has been used to estimate temperature shocks,[4] its application in analyzing the agriculture/weather nexus is relatively recent. LPs enable the tracing of the response of agricultural production to weather shocks over various time horizons. They are particularly well suited for this purpose to account for non-linear seasonal effects, which are not readily apparent using annual data.

Our final contribution concerns the role of local weather shocks in triggering aggregate fluctuations. Instead of focusing on the channel of impact directly on aggregate outcomes, as in the literature,[5] we aggregate in-sample responses of regional crop production to weather shocks from LPs to build a macroeconomic index of weather shock losses. We then include this new index into an otherwise standard vector autoregressive model to quantitatively assess how weather shocks drive macroeconomic fluctuations.

The remainder of this article is organized as follows. Section 2 describes the data and the variables used in the empirical analysis. Section 3 details the estimation strategy and discusses the panel estimation results. Section 4 examines the differentiated effects of weather shocks across production stages, distinguishing between a growth regime and a harvest regime. Section 5 shifts the focus from agricultural production and investigates the transmission of weather shocks to the rest of the nation's economy. Section 6 provides a conclusion.

[3] To study long-term effects, Burke and Emerick (2016) suggest a framework in which they model the change in average yields at two different points in time for a given location as a function of changes in average temperature.

[4] Natoli (2022) applied this method to analyze the impact of temperature surprises on the US economy using quarterly data.

[5] See, for example, Acevedo et al. (2020), who identify negative impacts of weather shocks on agricultural and aggregate output in developing countries.

2 Data

This section summarizes the main data sources used in the empirical analysis as well as the data transformation process used to compute abnormal weather shocks and their mapping to deseasonalized agricultural production data.

2.1 Regional Agricultural Production Data

Our primary source of agricultural data is derived from monthly agricultural reports, *El Agro en Cifras*, produced by the Ministry of Agriculture and Irrigation of Peru (MINAGRI) spanning from 2001 to 2019.[6] These reports provide agroeconomic indices and agricultural production figures at both regional and national levels. We extracted data on production (measured in tons) and on the planted and harvested areas (measured in hectares) for each of the primary crops cultivated in Peru across 25 administrative regions, covering the period from January 2001 to December 2015. It is important to note that observations after 2016 are no longer reported on a monthly basis but are presented quarterly; therefore, they are excluded from our analysis. Each monthly report presents data as a cumulative sum from January to the respective reporting month. To convert the production data into net flows, we apply a first-difference filter.

Four main crops are analyzed in this study: potato (*papa*), cassava (*yuca*), rice (*arroz cáscara*), and maize (*maíz amarillo duro*).[7] The selected crops in this study collectively represent a substantial share of agricultural production, comprising 53% of the cultivated surface and 37% of the total production in Peru.[8] To ensure the validity of our data over the same years of observation, we cross-referenced them with the Food and Agriculture Organization data (FAOSTAT) and, observed similar quantities (see Table C.1 in the appendix). According to the FAO data, the crops we focus on constitute 41% of the cultivated surface and 31% of the total quantity produced. The slight differences observed between the figures provided by the monthly reports produced by the Peruvian Ministry and those reported by the FAO are ascribed to the fact that the former focus solely on the main crops, while the latter are more exhaustive.

In agricultural economics, it is common to express agricultural production as yields by dividing it by the planted land surface. However, with monthly data, a significant number of observations exhibit zero values for the planted area, resulting in an inability to calculate yields for those months. In this article, we propose expressing

[6] The data can be downloaded from: https://www.midagri.gob.pe/portal/boletin-estadistico-mensual-el-agro-en-cifras.

[7] Two types of maize are reported in the MINAGRI reports. In the rest of the article, we refer to "Dent corn" as "Maize."

[8] While the Peruvian agricultural report includes data for other crop types, these exhibit numerous missing observations and do not encompass a sufficiently large time span for inclusion in the quantitative analysis.

agricultural production as a percentage deviation from the average. The advantages of this procedure are twofold: first, it avoids the arbitrary exclusion of zero values for agricultural production; and second, it naturally corrects for the size effect stemming from regional heterogeneity in production. Our data transformation is performed in two steps: demeaning and detrending. The demeaning step consists of dividing the raw data points $y^{\text{raw}}_{c,i,m}$ by the sum of all raw data points for a given crop c, region i, and calendar month m (*e.g.*, all observations in January) over the entire period T: $y^{\text{demeaned}}_{c,i,m,t} = \dfrac{y^{\text{raw}}_{c,i,m,t}}{n_T \sum_{t=1}^{T} y^{\text{raw}}_{c,i,m}}$. Next, a quadratic trend is estimated using ordinary least squares (OLS) regression: $y^{\text{demeaned}}_{c,i,m} = \beta_{c,i,m}t + \gamma_{c,i,m}t^2 + \varepsilon_{c,i,m}$, where $\varepsilon_{c,i,m}$ represents the error term assumed to be normally distributed. The residuals represent detrended data:

$$y_{c,i,m} = y^{\text{demeaned}}_{c,i,m} - (\widehat{\beta}_{c,i,m}t + \widehat{\gamma}_{c,i,m}t^2), \tag{1}$$

where $\widehat{\beta}_{c,i,m}$ and $\widehat{\gamma}_{c,i,m}t^2$ are OLS coefficients. The detrended values can then be expressed in log form, where $y_{c,i,t}$ is the percentage deviation of agricultural production of crop c at time t harvested in region i.

2.2 Regional Weather Data

The selection of weather variables for inclusion in the analysis has received considerable attention in the literature. Given that the dependent variable is typically observed annually, the temporal aggregation of weather data is necessary.[9] Ortiz-Bobea and Just (2012) notes that most econometric models rely on weather variables aggregated over the growing season with the underlying assumption that growing season dates are fixed in time. In this vein, some studies have defined accumulated metrics over the growing season, such as growing degree days (Schlenker and Roberts, 2009). Other studies segment the growing season into several parts, based on the four seasons (Schmitt et al., 2022), or weeks of the year (Powell and Reinhard, 2016). The division of the periods can also be performed to match the different stages of the growth process, such as the vegetative phase, ripening, and maturation (Ortiz-Bobea et al., 2019; Welch et al., 2010). The consideration of multiple points in time for aggregating weather variables stems from the idea that weather shocks can impact agriculture differently, depending on when they occur. However, even when weather data are aggregated across the different stages of production, the annual nature of the response variable prevents the study of intra-season dynamics of the effects of weather shocks. To address this issue, we use monthly data and local projections, which enable us to study

[9] The literature has also addressed the issue of spatial aggregation, which can lead to very different results, depending on the chosen method. For more details, please refer to D'Agostino and Schlenker (2016).

these dynamic effects.

To construct the weather shock series, we consider daily grid temperature and precipitation data, aggregated at the monthly level for each of the 24 regions of Peru. We follow Barrios et al. (2010) and demean weather observations at the grid level. The means are the monthly historical values observed over the past 20 years. Next, we aggregate the values at the regional and monthly levels. The aggregation process is described in detail in this section. In summary, the obtained variables – temperature and precipitation anomalies – are deviations from the average.

Grid temperature data. We obtained data from PISCOt V1.1, a gridded daily temperature data set available for Peru. The data were collected from January 1981 to December 2016. The grid has a 0.1° spatial resolution (10 km). The data set is developed by the SENAMHI (the National Service of Meteorology and Hydrology of Peru). The methodology that led to the construction of this data set is explained by Huerta et al. (2018).[10]

Grid precipitation data. The rainfall data are obtained from the CHIRPS v2.0 database, made available by the Climate Hazards Center of the UC Santa Barbara. Covering almost the entire globe, the data set provides daily information on rainfall on a 0.05° resolution satellite imagery, from 1981 to the present. The complete presentation of the data can be found on the Climate Hazards Center website (Funk et al., 2015) and the dataset is freely available online.[11]

From grid data to regional data. Agricultural production is available at the regional level. Therefore, it is necessary to map grids and regions to aggregate the weather data at the regional level. In addition, shocks such as excessive temperatures or rainfall occurring in agricultural areas should not be accounted for in the same way as shocks occurring in urban geographic land. For example, the weather conditions of a grid cell where 90% of the surface is used for agricultural production should matter more than those of a cell with 10% of the agricultural surface. When aggregating the weather data, we must identify where agricultural regions are located in Peru to give these regions more weight in the aggregation procedure. To do so, we rely on data from Copernicus, a European program for monitoring the Earth using satellite and *in situ* data managed by the European Commission.[12] We use the 2015 Peru data with a 100m resolution.

[10]Data can be obtained from https://drive.google.com/drive/folders/1eGqhmJXBJfFSzUFz2RVqtbKIlOphpkcs.

[11]See https://data.chc.ucsb.edu/products/CHIRPS-2.0/.

[12]The data are freely available: https://land.copernicus.eu/global/products/lc. The share of agricultural land for each grid cell is shown on the map in Figure 2 in the Online Appendix.

Regional weather anomalies. What are the relevant weather shocks for predicting agricultural production? Parry et al. (2007) documented a large negative sensitivity of crop production to extreme daytime weather variables. We build on this observation to construct our temperature variable by computing the average monthly maximum temperature. The precipitation variable is defined as the sum of the monthly rainfall. Following D'Agostino and Schlenker (2016), transformations of the weather data are first performed at the scale of the cells of the grid and then aggregated at a monthly frequency for each region. Let $\mathcal{T}_{c,y,m,d}$ and $\mathcal{P}_{c,y,m,d}$ denote the temperature and precipitation observed in cell c on day $d = \{D1, D2, ...D31\}$, month $m = \{M1, M2, ...M12\}$ and year $y = \{2001, 2002, ..., 2015\}$. The temperature variable denoted $\mathcal{T}_{c,y,m}$ is defined here as the average of the most extreme meteorological events observed over the sequence of days within the considered month m in cell c, whereas the precipitation variable denoted $\mathcal{P}_{c,y,m}$ is defined as the sum of the observed daily values:

$$\mathcal{T}_{c,y,m} = \frac{1}{N_d} \sum_{d=1^{N_d}} \mathcal{T}_{c,y,m,d}, \quad \mathcal{P}_{c,y,m} = \sum_{d=1^{N_d}} \mathcal{P}_{c,y,m,d},$$

where N_d is the number of days within month m.

We measure the distance of the weather variable from its monthly average to assess the relative intensity of one weather shock with respect to the other realizations. Let $\mathcal{W}_{c,y,m}$ denote one of the two weather measures, temperature or precipitation, observed in cell c, month m and year y. The abnormal realization of the weather is expressed as follows:

$$W_{c,y,m} = \mathcal{W}_{c,y,m} - \overline{\mathcal{W}}_{c,\bullet,m},$$

where $\overline{\mathcal{W}}_{c,\bullet,m} := (y_T - y_0 + 1)^{-1} \sum_{y=y_0}^{y_T} \mathcal{W}_{c,y,m}$ denotes the average value of the weather data in cell c observed during a specific month m from year y_0 to year y_T. We set $y_0 = 1986$ and $y_T = 2015$ so that the average is computed over a period of 30 years, which is a standard practice in the literature to define climate normals (see, *e.g.*, Deschênes and Greenstone, 2007; Auffhammer et al., 2013).

Cell-specific weather anomalies are then aggregated at a monthly regional level. To accomplish this, for each region, we simply calculate the average of the anomalies from each cell, weighting each term according to two measures. The first is the proportion ω_c^{area} of the cell to the total surface area of the region. The second is the proportion $\omega_c^{\text{cropland}}$ that the cell represents in the agricultural production of the region.

The weather anomaly variable is defined at each date t (year y and month m) as follows:

$$W_{i,t} = \frac{\sum_{c \in \mathcal{R}_i} \omega_c^{\text{area}} \omega_c^{\text{cropland}} W_{c,t}}{\sum_{c \in \mathcal{R}_i} \omega_c^{\text{area}} \omega_c^{\text{cropland}}},$$

where $\mathcal{R}_i$ denotes the set of cells that fall in region i.

We apply this procedure to both temperature and precipitation observations to derive the temperature anomaly $T_{i,t}$ and the precipitation anomaly $P_{i,t}$ in region i at time t. We interpret a large value of $T_{i,t}$ as excess heat (measured in ℃) with respect to its historical average. Similarly, we interpret a large value of $P_{i,t}$ as an excess humidity (measured in millimeters of rain) with respect to its historical average.

2.3 ENSO Oscillations

To explore the cause-and-effect relationship, local projections are typically built under the assumption that weather shocks (or any regressor of interest) are unexpected. However, our sample also includes El Niño and La Niña events. Notably, these climate phenomena are characterized by their predictable occurrence, diverging from the typical unexpected nature of weather shocks. Even though farmers are still surprised by the magnitude of the weather shocks during ENSO events, they can adapt by adjusting their crop mix before the weather shock materializes, introducing a potential bias in the quantitative analysis. To circumvent this issue, we use ENSO variations as a control variable to account for the expectational effect that ENSO may have on the projection. These ENSO fluctuations are classified using the Oceanic Niño Index, which computes a three-month average of the sea surface temperature anomalies in the central and eastern tropical Pacific Ocean. We collect this index from the Golden Gate Weather Service.[13] An El Niño (or La Niña) event is defined by a period of five consecutive three-month periods with an index above 0.5 (or below -0.5 for a La Niña event).

2.4 Macroeconomic Data

Because the data-generating process of our agricultural data is driven by alternative sources of randomness, such as economic shocks unrelated to the weather, we include macroeconomic data as control variables. The goal of this control variable is to isolate the effect of weather variables on agricultural production from any other sources of fluctuation. By holding constant values for the control variables, any changes in the outcome can be attributed solely to the variable of interest, rather than the combined effects of multiple variables. This makes it possible to draw more accurate conclusions regarding the causal relationship between weather shocks and agricultural output. To consider these potential effects, control variables based on macroeconomic data for the Peruvian economy taken from the data warehouse of *the Banco Central de Reserva del*

[13] See https://ggweather.com/enso/oni.htm.

Peru are included.[14] More specifically, the following series are included: the Peruvian Consumer Price Index (CPI), Food Price Index (FPI), Sol/US Exchange rate, national interest rate, GDP index and a sectoral index for industrial production. Note that all the control variables are national aggregates given on a monthly basis. Nominal variables (*e.g.*, exchange rate, FPI, and CPI) are detrended by calculating the growth rate. GDP and industrial production indices are expressed as percentage deviations from the Hodrick-Prescott filter to control our projections from the effects stemming from aggregate demand and supply shocks. A similar transformation is applied to the interest rate, as the latter exhibits a downward trend in the considered time span. In addition, we control for international variations that may affect the production of each culture by including their respective commodity prices using data from the International Monetary Fund.[15]

2.5 Summary Statistics of Agricultural Data

This section introduces the primary features of the dataset. Table 1 presents descriptive statistics for the monthly production of the selected crops averaged over the regions. One can observe an important variation in production, which is highly crop-specific. We remove the negative values for production from our data, attributable to different revaluations of production data estimates. We also exclude regions where no tons were produced during the sample period. Columns 7 and 8 report the number of producing regions and observations, respectively, for each type of crop.

In addition to this table, Figure 1 provides a visual representation of the national production of crops over our time sample, which is the sum of monthly regional production. Interestingly, some cultures exhibit a clear and regular pattern (such as potato and rice), whereas others are more volatile. We also observe a positive trend for cassava.[16] We consider these features in the following sections by deseasonalizing the data.

[14] Data are taken from the Central Bank of Peru, where the Real Exchange Rate token is *PN01259PM*, Exports is *PN01461BM*, Food CPI is *PN01336PM*, CPI is *PN01270PM*, industrial GDP is *PN02079AM*, GDP *PN01773AM*, and interest rate is *PN07819NM*. All seasonal components are removed from the time series, excluding the interest rates.

[15] International commodity prices have been taken from the IMF Primary Commodity Price System website.

[16] This positive trend is potentially due to the increase in agrarian land, resulting from deforestation of the Amazon rainforest, where a large share of cassava is produced. See Figure 3.

Culture	Mean	Median	Standard Deviation	Min.	Max.	No. regions	No. obs.
Cassava	6,004.5	3,878.0	7,792.5	0.0	16,079.9	15	2,631
Maize	7,169.7	4,336.0	8,490.5	0.0	2,704.6	13	2,271
Potato	17,252.1	5,801.0	30,155.5	6.0	360,070.0	12	2,091
Rice	13,127.7	4,441.3	16,212.9	3.9	8,863.4	7	1,212

Notes: Quantities are reported in tons.
Source: MINAGRI. Author's estimate

Table 1. Descriptive statistics for monthly production (in tons) per type of crop

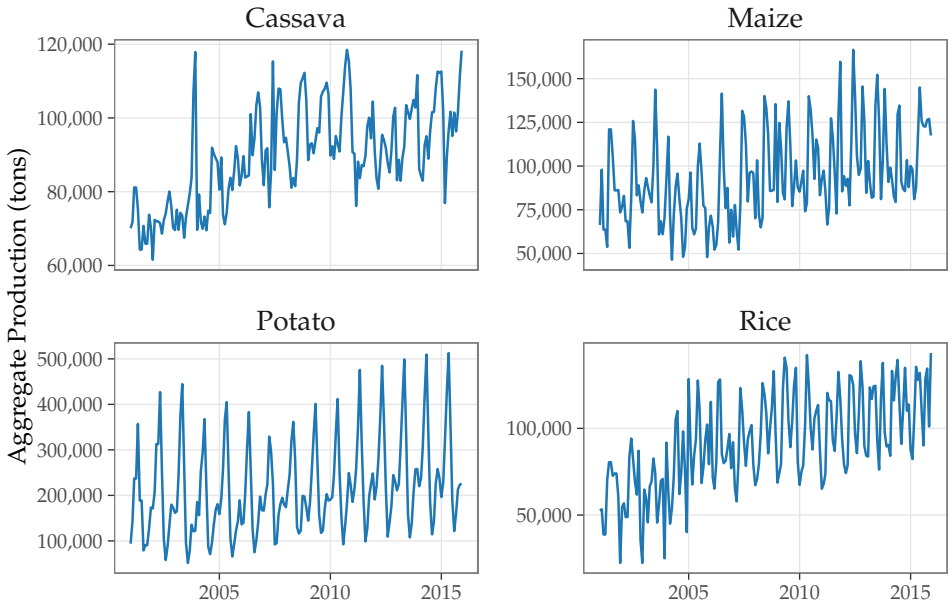

Notes: The graphs show the evolution of monthly crop production, summed over all administrative regions. For cassava, two observations (2007-06-01 and 2007-07-01) were identified as erroneous and replaced by a linear interpolation between May and July 2007.
Source: MINAGRI. Author's estimate

Figure 1. National monthly crop production for selected crops (in tons)

Peru is geographically very diverse in terms of climate and geographical topology, and is usually divided into three types of climate areas: coastal, highlands, and Amazon rainforest. These areas exhibit very different climatic conditions because of their proximity to the sea and their different altitudes. As explained by Aragón et al. (2021), the coastal area is a narrow strip extending from the seashore to 500 m above sea level (masl). It is situated in a semi-arid climate, with warm temperatures and little precipitation. The highlands extend from 500 masl to almost 7,000 masl, although most agriculture ceases below 4,000 masl. They have a much cooler and wetter climate, with seasonal precipitation in spring and early summer. Finally, the Amazon rainfor-

est area is continental and is characterized by tropical weather with significant rainfall. A map dividing the Peruvian territory into these three natural regions is provided in Figure C.2 in the Appendix, based on the data available on the Geo GPS Peru website.[17] Natural regions do not necessarily coincide with administrative regions. Consequently, for each region, three variables are constructed, indicating the share of each type of natural region in the administrative region.

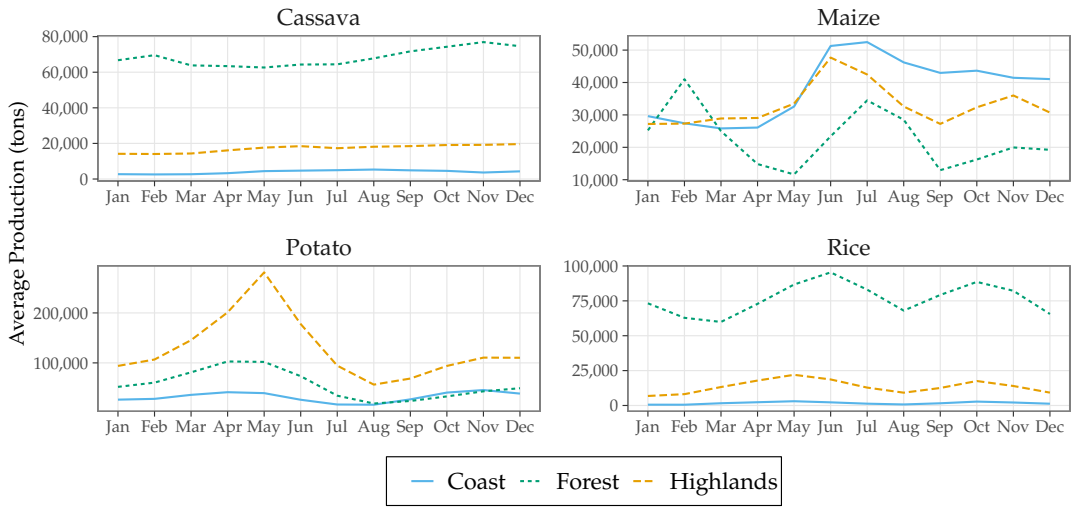

Notes: The graphs show the sum of each crop production, broken down by month and weighted by the share of the natural region.
Source: MINAGRI. Author's estimate

Figure 2. Crop production by months and natural regions (in tons)

In Figure 2, we document regional differences and seasonality by averaging monthly production over different types of natural regions. In these graphs, seasonal patterns are observed more closely. For example, potato production sharply increases between March and May before decreasing thereafter. In contrast, maize displays differentiated seasonal cycles, depending on the natural region. In coastal regions, we notice that there is only one production peak, in June. In forested areas, there are two main peaks: a high peak in February and a smaller peak in July. Finally, the example of cassava shows that production can be highly concentrated in one area, here, in the forest, where more than half of the production is located. In contrast, maize production is more evenly distributed. Figure 3 presents the geographical distribution of each type of crop production in detail. Striped areas are excluded from the analysis owing to the structure of the data. Some regions produce crops only for a few months. Therefore, the reported production in the other months is zero, which makes it difficult to study the propagating effects of a weather shock in these regions. As can be seen in the maps, only a small number of regions that produce potatoes and rice at a significant

[17] See https://www.geogpsperu.com/2019/11/mapa-de-regiones-naturales-costa-sierra.html.

level at the national scale are excluded. We account for seasonality in the data by deseasonalizing them, and investigate in more detail the differences in regional crop development in Section 4.

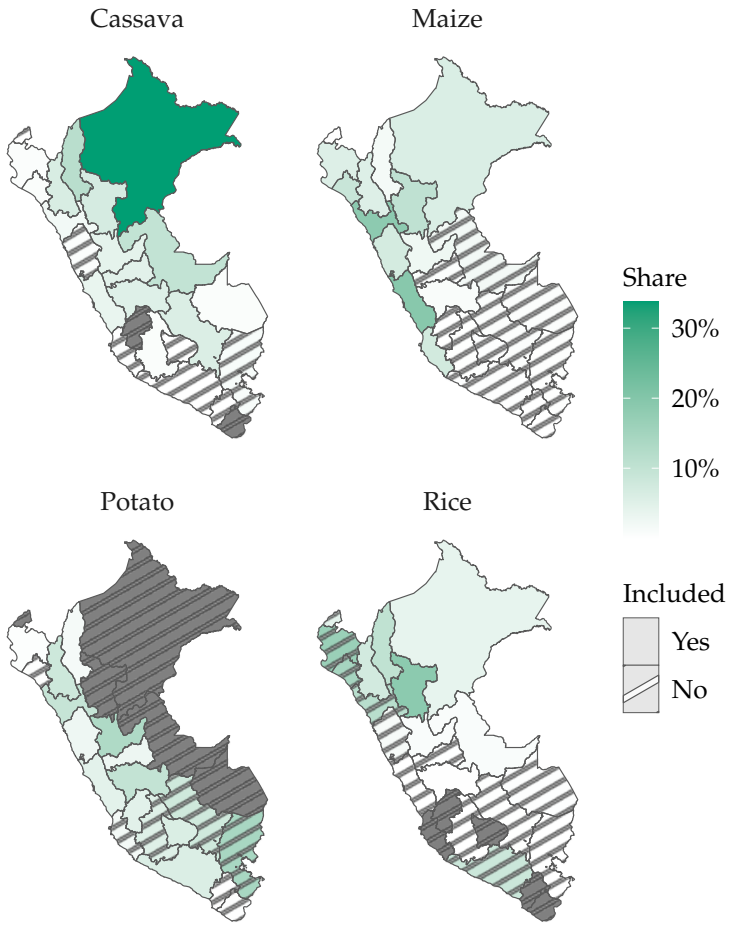

Notes: Distribution of production of each crop by administrative region. For each map, the sum of the distributions across regions equals 1. The non-producing regions are shown in gray.
Source: MINAGRI. Author's estimate

Figure 3. Regional distribution of crop production by administrative regions

3 The Dynamic Effects of Weather Shocks

How do weather shocks dynamically affect agricultural production? This section discusses the econometric approach and the main results obtained from the impulse response function analysis.

3.1 Empirical Approach

Our empirical framework follows a conceptual framework that is similar to that proposed by Dell et al. (2012). To fix ideas, consider the following simple economy char-

acterized by a Cobb-Douglas technology in the agricultural sector in region i for crop c:

$$Y_{c,i,t} = A_{c,i} N_{c,i,t} H_{c,i,t}, \tag{2}$$

where the agricultural output for crop type c planted in region i at time t is denoted by Y, crop-regional total factor productivity is denoted by A, labor demand is denoted by N and harvested area is denoted by H. Note that in this expression, $A_{c,i}$ captures how regional conditions, such as local labor productivity, shape the productivity of labor for crops planted in this region. By contrast, $N_{c,i,t}$ encapsulates macroeconomic fluctuations stemming from the labor market (*e.g.*, all aggregate shocks realized in t determine the country-wide real wage). Finally, $H_{c,i,t}$ represents the surface harvested with N units of labor.

How does the weather interfere within the production process of agricultural goods? Consider that each period, farmers in region i plant crop c on land surface L. A typical crop growth cycle implies a lag between planting and harvesting, referred to as the *growing season*. During the growing season, crops are vulnerable to weather shocks such as droughts and floods, leading to reduced growth and yield. In addition to these direct effects, weather shocks lead to increased stress in plants, making them more vulnerable to diseases. In severe cases, droughts can cause complete crop failure.

To capture these delayed effects of the weather on agricultural yields, let T_c denote the monthly duration of the crop-specific growing season between planting ($h = 0$) and harvesting ($h = T_c$). Therefore, it is assumed that $L_{c,i,t}$ units of planted land yield $L_{c,i,t} \exp(\sum_{h=0}^{T_c} \beta_{c,h} W_{i,t-h})$ effective units of productive land, where a weather shock $W_{i,t-h}$ realized in $t - h$ affects crop production harvested in t with elasticity $\beta_{c,h}$.[18] Weather shocks are considered from the farmer's perspective as exogenous variables that affect land productivity during the growing season. Weather variables, stacked in W, are formally connected to agricultural output as follows:

$$H_{c,i,t} \leq L_{c,i,t} \exp\left(\sum_{h=0}^{T_c} \beta_{c,h} W_{i,t-h}\right). \tag{3}$$

In this expression, it is assumed that the land surface planted $L_{i,c,t}$ exhibits both seasonal and trend components stemming from soil quality across time and space. Assuming that all planted surfaces are harvested, Equation 3 binds to equality. However, in the presence of severe weather shocks, if the marginal cost of harvesting exceeds the marginal profits of the land, it might be optimal for farmers to partially harvest the

[18] Note that we do not include a squared value for the weather variables. Squared terms are typically introduced to capture low-frequency effects of climate change. In this study, the time-frequency is monthly. The use of a squared term does not change the sign or significance of the results, as can be observed in the online replication materials.

planted surface.

Combining Equation 2 and Equation 3, and applying logs yields the following expression:

$$\ln\left(\frac{Y_{c,i,t}}{L_{c,i,t}}\right) = \ln\left(A_{c,i}\right) + \sum_{h=0}^{T_c} \beta_{c,h} W_{i,t-h} + \ln\left(N_{c,i,t}\right). \tag{4}$$

The left-hand side of this equation represents the percentage deviation of agricultural production from its potential value, measured by $L_{c,i,t}$.

A natural question at this stage is to gauge the importance of the elasticity of agricultural production to changes in weather conditions, namely, to infer the value of $\beta_{c,h}$. We use local projections based on Jordà (2005) to estimate the impact of weather shocks on agricultural output during the crop growing season. In this study, the two main exogenous variables are precipitation and temperature anomalies described in the data section. The advantage of local projections is that they allow for dynamic responses, while neither imposing the estimation of the entire autoregressive model nor introducing exogeneity restrictions.

To estimate these effects, we run a local projection for $h = \{0, 1, ..., T_c\}$ of the form:

$$y_{c,i,t+h} = \alpha_{c,i,h} + \beta^T_{c,h} T_{i,t} + \beta^P_{c,h} P_{i,t} + \delta_{c,i,h} X_t + \varepsilon_{c,i,t+h}, \tag{5}$$

where h is the time horizon. Consistent with Equation 4, agricultural production $y_{c,i,t+h}$ is deseasonalized and expressed as a percentage deviation from the trend.[19] Parameters $\alpha_{c,i,h}$ are the regional fixed effects that capture time-invariant factors, such as the local productivity level of labor or soil quality in region i. Additionally, the terms $T_{i,t}$ and $P_{i,t}$ represent the two distinctive weather variables that are considered in the inference exercise, namely, the temperature and precipitation anomaly variables (as detailed in Subsection 2.2). The two sequences of coefficients associated with the weather variables, $\beta^T_{c,h}$ and $\beta^P_{c,h}$, are of first order interest as they indicate how sensitive agricultural output is to exogenous changes in the weather variables. In addition, $X_t = [RER_t, r_t, \pi_t, y^{\text{ind}}_t, ENSO_t, \pi_{c,t}]$ is the set of control variables that captures the contributions from aggregate fluctuations, as stacked in the labor demand term in Equation 4. The control variables include the Real Exchange Rate (RER_t) and the nominal interest rate (r_t), both expressed as the deviation from the trend calculated by the HP filter, the inflation rate (π_t), the seasonally adjusted industrial production index (y^{ind}_t) expressed as a percentage deviation from the trend calculated by the HP filter, the Oceanic Niño Index ($ENSO_t$), and the monthly international price variation of each crop ($\pi_{c,t}$). The set of coefficients $\delta_{c,i,h}$ is unknown and must be estimated in the

[19] Recall that OLS regression is employed with seasonal fixed effects and a quadratic trend to infer the potential production of crops measured by $L_{c,i,t}$ in Equation 4.

inference exercise. Finally, $\varepsilon_{c,i,t+h}$ is an error term assumed to be normally distributed with zero mean.

3.2 Impulse Response Functions Results

The estimated coefficients in Equation 5 are multiplied by the standard deviation of the weather variable to obtain the impulse response of agricultural production to a standard weather shock. The responses are reported in Figure 4 for a nine-month horizon, contrasting for the four different crops considered. A response to a one standard deviation shock of temperature anomalies is reported at the top and for precipitation anomalies at the bottom.[20] In both cases, a positive shock is considered: a one standard deviation increase in temperature and a one standard deviation increase in precipitation, both with respect to their historical averages. Positive deviations in temperature or precipitation anomalies correspond to higher-than-usual values.

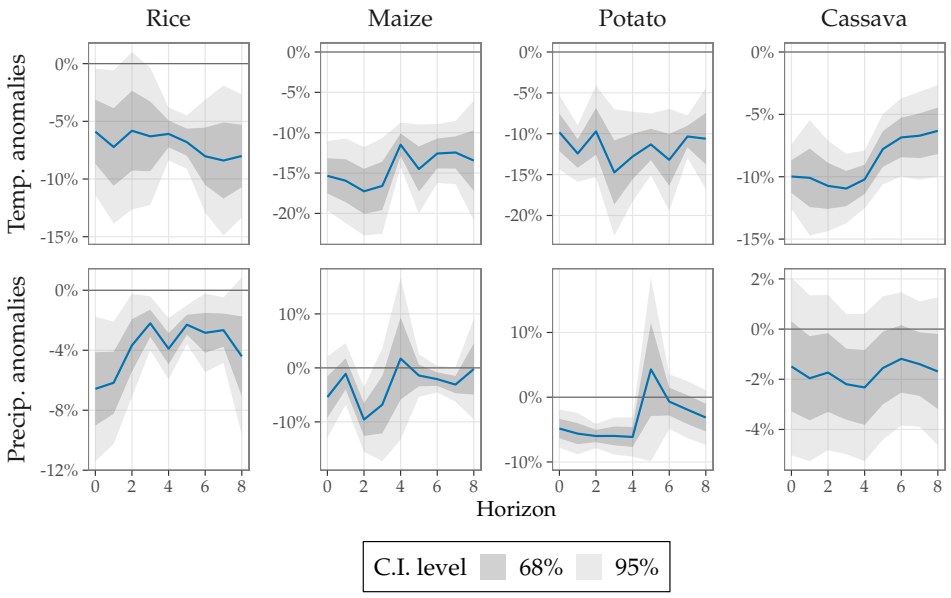

Notes: The panels show the crop-specific impulse response function of monthly agricultural production to a one standard deviation (SD) increase in the weather variable, which is defined as a 1 SD increase with respect to the historical average. The weather variables are the temperature anomaly in the first row and the precipitation anomaly in the second row. Horizon 0 represents the month of the shock. The shaded areas represent the 95% and 68% confidence intervals with region-level clustered standard errors.
Source: Author's estimates.

Figure 4. Agricultural production response to a weather shock

Overall, the shock leads to a sharp and net decrease in production for several months for every crop considered in our sample. However, the response is crop-specific because of the heterogeneous characteristics of the four types of crops considered. In

[20] Note that the number of regions is not the same across crops because some regions do not produce specific types of agricultural products. We refer to Table 1 for a description of agricultural production per region and crop type.

terms of magnitude, maize production appears to be the most affected by a temperature shock, with a loss of 15% of the detrended production after a rise in the monthly maximal temperatures of one standard deviation with respect to the historical average. The effect of the shock lasts for several months, and production remains highly altered eight months later. The fact that IRFs do not necessarily return to zero after harvesting underscores a learning mechanism. Farmers adjust their agricultural practices in response to realized weather shocks, making permanent modifications to their choice of crops or land usage. In contrast, while the production of cassava is also highly affected by a temperature shock, resulting in an immediate loss of 10% of the production, it exhibits a faster recovery compared to the other crops. It begins to rebound four months after the shock. Rice exhibits a smaller, albeit more persistent, decrease in production, suggesting that this crop type is more temperature-tolerant.

The second row of panels in Figure 4 reports the response of agricultural production following the realization of a precipitation anomaly shock at $h = 0$. A positive realization of the shock is associated with wetter than usual weather, more specifically, a one standard deviation increase in total precipitation relative to the historical average. A precipitation anomaly exhibits a similar pattern with respect to temperature anomaly shocks but with a response of a relatively smaller magnitude. Excess rainfall is detrimental to agricultural production, leading to an average agricultural loss between 2% and 10% with stronger effects occurring a few months after the shock. As explained by Skees et al. (2007), El Niño events in Peru devastated several regions with massive flooding that washed crops away.[21] The presence of a tropical climate, characterized by abundant rainfall, induces a large decrease in agricultural production following the realization of the precipitation anomaly shock. Although the shocks display a similar pattern, each crop reacts differently to them through the timing and magnitude of their responses.

Variations in production following a precipitation shock are also highly crop-specific and more volatile than responses to temperature shocks. Rice and potatoes are clearly affected during the first months following the shock, and the effect becomes more variable and less significant. Maize and cassava, although highly sensitive to temperature shocks, show small and more volatile responses to abnormally high precipitation.

4 Time-varying Exposure to Weather Shocks

The baseline projections in Section 3 underline the fact that the impact of weather shocks is relatively stronger in the months following the occurrence of the shock.

[21] Crost et al. (2018) find that an increase in wet-season rainfall is harmful to crops and produces more conflict in the Philippines.

However, the response also exhibits long-lasting effects of weather shocks, implying that not only the crops ready to be harvested, but also those that are still growing are affected. Thus, a natural question that arises from this observation is to investigate when the shock has a more significant impact.

A significant body of literature has demonstrated that the impact of weather shocks on agriculture depends crucially on crop growth stages. For instance, Welch et al. (2010) shows differential effects of increases in minimum and maximum temperatures on rice yields in tropical/subtropical Asia based on the growth phase. Additionally, Letta et al. (2022) finds that weather shocks trigger a rise in food prices during the growing period. Moreover, Massetti et al. (2016) empirically examines how weather shocks during a growing season affect maize and soybean harvests using US county-level data. Crops necessitate different types of nutrients depending on the stage of plant development. Excessively high temperatures or water volumes can be highly detrimental to crop growth at some stages while having little or no effect at other stages. This section aims to capture this effect. We leverage the high frequency of the data to monitor the quantity of crops planted and harvested each month. Departing from the conventional approach of using growing versus harvesting season dummies in annual data analysis, our measure of the growing season is a monthly continuous variable that weighs the flow of land planted versus harvested. Although it is not possible to identify each developmental stage with the available data, we can distinguish the growing period (i.e., when the planted surface is increasing) from the harvesting period (i.e., when the harvested surface is increasing). The response of agricultural production to weather shocks can be contrasted between planted and harvested regimes. To achieve this using local projections, we adapt the framework developed by Auerbach and Gorodnichenko (2011) for fiscal policy, modifying it to accommodate state-dependent effects of the weather with a smooth transition between the growing and harvesting stages.

4.1 A State-dependent Framework

Recall the toy model of agricultural production from Equation 3. In this section, we modify this model to endogenize plant crop decisions.

Let $p_{c,i,t}$ denote the new surface planted and $h_{c,i,t}$ denote its harvested counterpart at time t for crop type c in region i. Therefore, the net flow of the newly planted surface is given by $p_{c,i,t} - h_{c,i,t}$. The total fraction of land with growing crops is measured here as the cumulative sum of flows in the cultivated land surface over the lifetime of a crop T_c as follows: $z_{c,i,t} = \sum_{h=0}^{T_c} (p_{c,i,t-h} - h_{c,i,t-h})$. To compare regions on a regular basis, we remove the possible trend and divide by the standard error as follows, $\hat{z}_{c,i,t} = (z_{c,i,t} - z^{HP}_{c,i,t})/\sigma_{c,i,t}$, where $\hat{z}_{c,i,t}$ is the zero-mean standardized index variable of the utilized land surface. To express this index as a transition function with support

[0,1], since the planted surface index has been standardized, $\hat{z}_{c,i,t} \sim \mathcal{N}(0,1)$, we use the cumulative distribution function of the standard normal distribution $\Phi(\cdot)$:[22]

$$\Phi(\hat{z}_{c,i,t}) = \frac{1}{\sqrt{2\pi}} \int_{-\infty}^{\hat{z}_{c,i,t}} \exp(-t^2/2)\, \mathrm{d}t. \tag{6}$$

Letting $\Phi(\hat{z}_{c,i,t})L_{c,i,t}$ denote the fraction of the potential land that is planted, $\Phi(\hat{z}_{c,i,t})$ is interpreted as the mass of land planted or the degree of exposure of agricultural production to weather changes.

Consider now that weather effects depend on the growth stage of crops. The harvesting season is interpreted as the period when the mass of land planted $\Phi(z_{c,i,t})$ is low (approaching zero). By contrast, the growing season corresponds to a situation in which $\Phi(z_{c,i,t})$ is high (approaching one). In contrast to the effects of the weather on the growing and harvesting seasons, the surface of harvested land can be written as follows:

$$H_{c,i,t} \leq L_{c,i,t} \exp\left(\sum_{h=0}^{T_c} \left(\Phi(\hat{z}_{c,i,t-h})\beta_{c,G}^{h} + (1 - \Phi(\hat{z}_{c,i,t-h}))\beta_{c,H}^{h} \right) W_{i,t-h} \right), \tag{7}$$

where $\beta_{c,G}^{h}$ and $\beta_{c,H}^{h}$ are agricultural production responses during the growing and harvesting seasons, respectively.

Injecting this term into the production yields to the following expression:

$$\ln\left(\frac{Y_{c,i,t}}{L_{c,i,t}}\right) = \ln\left(A_{c,i}\right) + \sum_{h=0}^{T_c} \left(F(\hat{z}_{c,i,t})\beta_{c,G}^{h} + (1 - F(\hat{z}_{c,i,t}))\beta_{c,H}^{h} \right) W_{i,t-h} + \ln\left(N_{i,c,t}\right). \tag{8}$$

The local projections framework can be accommodated again to analyze the role of the growing versus harvesting season in the propagation of shocks. We examine the non-linear influence of the season on the response of each crop production to weather shocks. The same local projection method is used, but augmented with a state-dependent variable to allow for non-linear responses as described in Auerbach and Gorodnichenko (2011). This framework considers the probability of being in the

[22] Note that Auerbach and Gorodnichenko (2011) adopt a similar strategy to define recessions but assume a logistic transition function, which implies having to arbitrarily define a threshold when calibrating the parameters of the logistic function. To avoid this assumption, we use the cumulative distribution function of the standard normal distribution.

growing season or during the harvesting season:

$$y_{c,i,t+h} = \Phi\left(\hat{z}_{c,i,t}\right)\left[\alpha^{G}_{c,i,h} + \beta^{G,T}_{c,h} T_{i,t} + \beta^{G,P}_{c,h} P_{i,t} + \delta^{G}_{c,i,h} X_t\right] + \left(1 - \Phi\left(\hat{z}_{c,i,t}\right)\right)\left[\alpha^{H}_{c,i,h} + \beta^{H,T}_{c,h} T_{i,t} + \beta^{H,P}_{c,h} P_{i,t} + \delta^{H}_{c,i,h} X_t\right] + \varepsilon_{c,i,t+h}, \quad (9)$$

where $y_{c,i,t+h}$ is the deseasonalized production, and $T_{i,t}$, $P_{i,t}$, and X_t are, respectively, the temperature anomalies, precipitation anomalies, and control variables, as previously defined in Equation 5. The difference from this latter equation is that we now estimate the associated coefficients conditionally on the state of the season. Note that $\beta^{H,T}_{c,h}$ and $\beta^{H,P}_{c,h}$ are, therefore, the parameters of interest for the harvesting season, whereas $\beta^{G,T}_{c,h}$ and $\beta^{G,P}_{c,h}$ are the parameters for the growing season. Following Auerbach and Gorodnichenko (2011), we also allow for seasonally dependent fixed effects and marginal effects for the control variables.

4.2 Season-dependent Impulse Response Functions

Figure 5 reports the response obtained from Equation 9. As before, the first row presents the crop-specific responses to a one standard deviation temperature anomaly shock, whereas the second row shows the responses to a precipitation anomaly shock. Responses are distinguished by regime: the gray line represents the responses during the growing season, while the green line refers to the harvesting season. Confidence intervals are reported at the 95% confidence level.

The distinction between growing and harvesting seasons plays an important role. Overall, we observe a differentiated impact, with a stronger reduction in production when a shock occurs during the growing season. This result appears more clearly when examining temperature shocks, whereas precipitation shocks display a more volatile response.

Two results are important to notice with this specification. First, looking at the responses to temperature shocks, we observe that both the magnitude and duration of the shock differ depending on its timing. More specifically, using the examples of rice and maize, it can be observed that production first decreases when a shock occurs during the harvesting season, but the effect vanishes over the months. This indicates that some of the production may have been damaged immediately prior to harvest. By contrast, when the shock occurs during the growing season and production decreases instantaneously, the strongest reduction occurs several months after the shock. This result suggests that not only is the grown part of the crop affected by the shock but also that the growing stage suffers from the shock. This result is in line with Hatfield and Prueger (2015) who find that when a temperature shock occurs during the growth

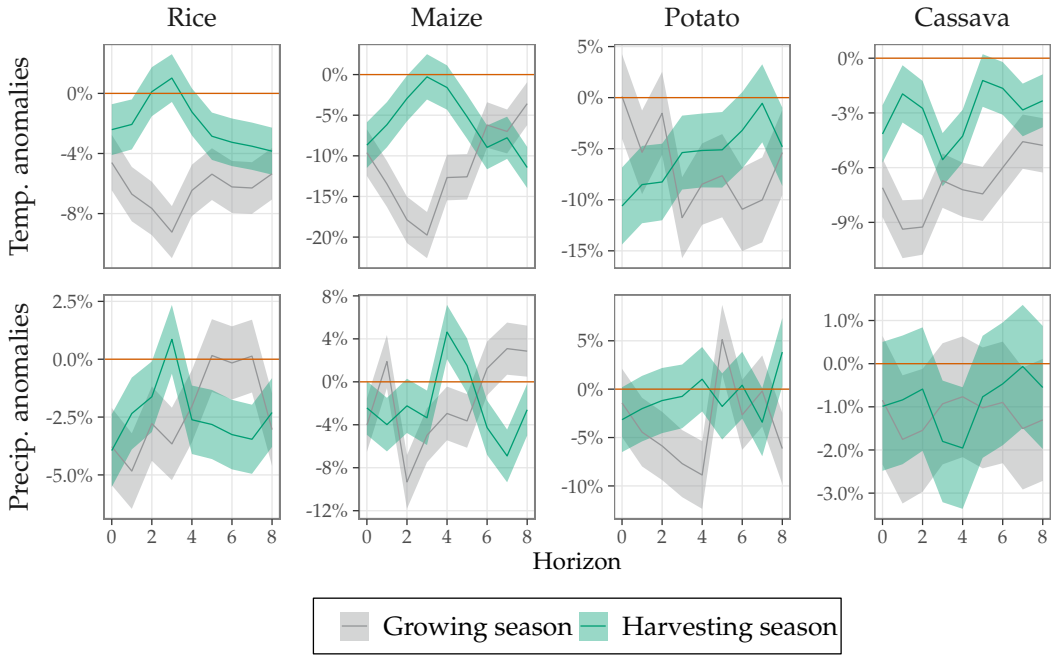

Notes: The panels show the crop and season-specific impulse responses of monthly agricultural production to a 1 SD increase in the weather variable. The weather variables are the temperature anomaly in the first row and the precipitation anomaly in the second row. Horizon 0 represents the month of the shock. The bands formed by the grey and green areas represent the 95% confidence intervals with standard errors clustered at the regional level for the growing season and harvesting season regimes, respectively.

Figure 5. Agricultural production response to a weather shock contrasting for growing vs. harvesting season

stage of crop development, it may affect crop growth, which in turn leads to lower yields. However, if a shock occurs when the crop is about to be harvested, then only a high magnitude shock (severe drought, hail, landslide, etc.) is likely to significantly affect production.

Strikingly, this effect is common to all cultures, although its timing and duration remain highly crop-specific. This underscores the importance of considering the different effects of season, which may not appear clearly when looking at aggregated variations over time. Because the seasons may vary slightly between regions (as shown in Figure 2), estimating the aggregated effect of weather shocks, as in Section 3, may undervalue the duration of the shock and thus provide a lower bound of the potential regional effects. Given that the responses differ with respect to season, policies designed to mitigate the aftermath of a shock should be adapted accordingly.

5 From Regional to Aggregate Fluctuations

Are regional weather shocks sufficiently important to spread to the rest of the economy? Weather shocks tend to be serially correlated across regions because these re-

gions share common atmospheric, soil, or topographic patterns. Therefore, a weather shock may entail macroeconomic fluctuations if the number of regions affected by the same weather pattern is high enough. On policy grounds, a quantitative assessment of weather shocks to macroeconomic fluctuations is particularly important for the design of mitigation policies.

5.1 Extracting the Weather Component of Agricultural Loss (WCAL)

The literature typically provides a synthetic measure of the weather based on average measures of county-level weather shocks and analyzes its interaction with macroeconomic time series (see, *e.g.*, Natoli, 2022; Gallic and Vermandel, 2020). This approach typically infers an immediate effect of a contemporaneous weather shock in t on macroeconomic variables, and its delayed reverberation through the propagation patterns over $t+N$ with N horizon. This methodology arbitrarily forces weather shocks to have immediate and homogeneous impacts on agricultural production, underestimating both (i) the delayed effects from the crop growth process, and (ii) the heterogeneous responses*of different crops.

By contrast, we propose measuring the macroeconomic effects of the weather through a "weather-implied losses" variable, as measured by our baseline local projections in Equation 5. We define the national weather-adjusted agricultural production y_t^{ω} at time t by summing the significant crop-specific contributions of weather represented by the coefficients of the weather variables $\beta_{c,h}^{T}$ and $\beta_{c,h}^{P}$ over the horizons and regions:[23]

$$y_t^{\omega} = \frac{1}{\sum_c \omega_{c,t}} \sum_c \sum_h \sum_i \frac{\mathbb{1}_{\text{signif}_{c,i,t,h}} \times \left(\beta_{c,h}^{T} T_{i,t-h} + \beta_{c,h}^{P} P_{i,t-h}\right) \times \omega_{c,t}}{\text{card}(I_{c,t})}, \tag{10}$$

where $\omega_{c,t} = \sum_i y_{c,t,i}^{\text{raw}} \times p_c$ is a quantity weight for crop c at time t. It represents the sum of monthly agricultural production over regions, expressed in monetary terms, where p_c is the average selling price of crop c in our sample. $\text{card}(I_{c,t})$ is the number of regions that produce crop c at time t, and the characteristic function $\mathbb{1}_{\text{signif}_{c,it,h}}$ equals 1 when the contribution is significantly different from 0 (based on the 95% confidence intervals of the coefficients $\beta_{c,h}^{T}$ and $\beta_{c,h}^{P}$), and 0 otherwise.

The national weather-adjusted agricultural production is then expressed as a measure denoted $WCLA_t$, termed the "weather component of agricultural losses."

$$WCLA_t = -100 \times (y_t^{\omega} - \overline{y_t^{\omega}}). \tag{11}$$

[23] The steps to obtain the expression of this variable are detailed in Appendix B.

This metric represents the deviation or loss from the expected trend. The trend itself is determined through the application of an HP filter. The inclusion of a negative sign ensures that positive values of $WCAL_t$ correspond to losses, rather than gains. In simpler terms, $WCAL_t$ provides an intuitive measure that expresses the percentage loss of agricultural value-added attributed to weather shocks.

5.2 A Vector Auto-Regression (VAR) approach

A vector auto-regressive (VAR) model is a straightforward way to quantitatively assess dynamic interactions across time series. A typical VAR model with p lags is:

$$Y_t = \phi_0 + \sum_{i=1}^{p} \phi_i Y_{t-i} + \varepsilon_t, \tag{12}$$

where Y_t is an $N \times 1$ vector of endogenous variables, ε_t denotes the error term, normally distributed with zero mean and variance Σ_ε, ϕ_0 is an $N \times 1$ vector stacking constant terms, and ϕ_i are $N \times N$ matrices gathering dynamic interactions across endogenous variables.

The vector of endogenous variables, $Y_t = \left[WCAL_t,\ RER_t,\ \pi_t^A,\ \pi_t,\ X_t,\ y_t^A,\ r_t,\ y_t \right]$, contains seven variables: the aggregate measure of weather-driven agricultural losses denoted $WCAL_t$, Real Exchange Rate (RER) denoted RER_t, the percentage change in the Food Consumer Price Index (CPIA) denoted π_t^A, the percentage change in the Consumer Price Index (CPI) denoted π_t, exports denoted X_t, agricultural production denoted y_t^A, GDP denoted y_t and nominal rate r_t. All macroeconomic data are presented in Subsection 2.4, except for the agricultural output, which is calculated using the regional monthly production values for the crops of interest $y_t^A = \sum_c \omega_{c,t}$, where $y_{c,t,i}^{\text{raw}} \times p_c$ is the quantity weight for crop c at time t from Equation 10. Variables exhibiting a trend (agricultural output and GDP) are expressed as percentage deviations from the Hodrick-Prescott trend, while seasonal components are removed using the X13 method of the Census Bureau. Our sample covers the period 2003M1–2015M12.

With the Cholesky factorization of the reduced-form VAR covariance matrix, the order of the variable matters. To impose full exogeneity in the weather process, we follow Gallic and Vermandel (2020) by placing the weather-driven agricultural-losses equation in the first position in the VAR and muting cross-interactions with other variables. Following the ordering scheme of Stock and Watson (2001), we next order price variables, followed by quantities, and terminate with interest rates. The idea is that price variables are driven more by exogenous factors (e.g., oil price shocks), whereas the interest rate is the most endogenous variable that reacts to contemporaneous changes in prices and quantities.

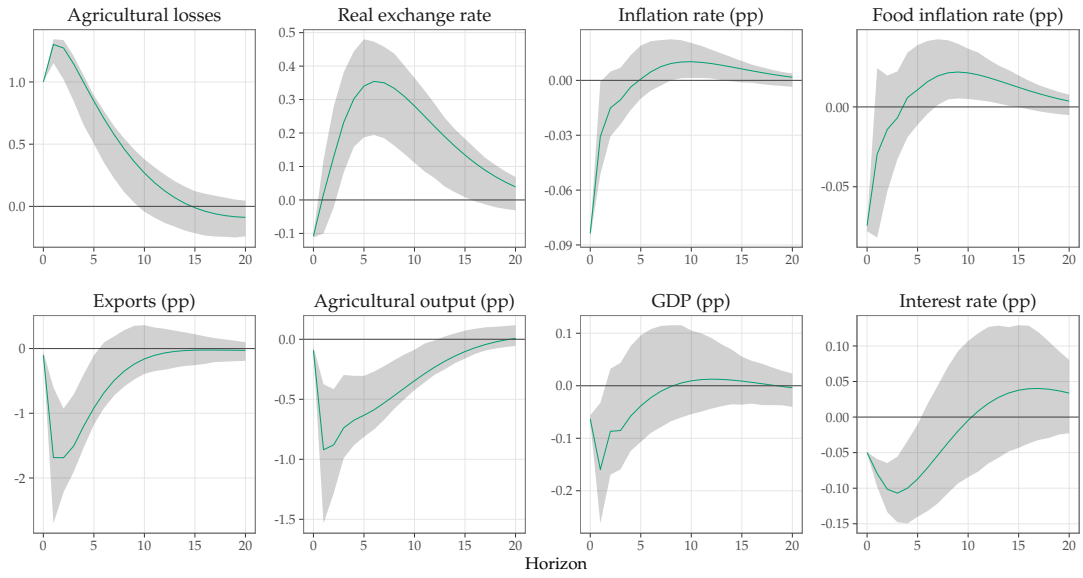

Notes: The solid blue line represents the Impulse Response Function. The gray band represents 68% error bands obtained from 500 Monte Carlo simulations. The response horizon is in months.

Figure 6. VAR(2) system response to an unit orthogonal shock to the weather aggregate cost equation

The number of lags selected using the AIC criterion is 2. Figure 6 illustrates the system's response to a unit increase in agricultural output resulting from weather shocks. An increase in losses in the agricultural sector due to weather shocks triggers an immediate 0.1% reduction in the real exchange rate, primarily because exports and outputs in the agricultural sector decrease. This overall recessionary impact leads to both consumer and food price indices decreasing initially, reflecting weak demand. The disinflationary effect of weather shocks aligns with the findings of Natoli (2022) and Faccia et al. (2021), both of whom observe lower-than-usual inflation following a temperature shock. However, it is important to note that our setup implies a positive inflation 10 months after the realization of the weather loss, which can be attributed to the scarcity of agricultural products.

In terms of quantities, a unit loss shock resulting from the weather implies a 0.9% reduction in agricultural output below its trend, while GDP is 0.15% lower. Finally, the central bank faces no trade-off on impact, as both prices and quantities are going in the same direction. However, after one year, when inflation picks up, a usual supply-driven trade-off emerges between inflation and quantity stabilization, as both move in opposite directions in medium term. The VAR model suggests that the Peruvian central bank prioritizes output stabilization when weather shocks occur, leading to a accomodative response of the nominal interest rate.

To connect our work with prior studies, our quantitative assessment of the macroeco-

nomic cost of weather shocks aligns with existing literature. The responses of output and interest rates closely mirror the findings of Natoli (2022) for the US economy regarding temperature anomalies. Additionally, our results are also consistent with the VAR model of Gallic and Vermandel (2020) for New Zealand, where they similarly observe a 0.1% decrease in GDP, a 1% decline in agricultural output, and a 0.4% drop in the real exchange rate following a drought shock.

6 Discussion and Conclusion

Much effort has been devoted in the literature to quantitatively measuring how the weather is an important driver of agricultural goods supply. This study contributes to this effort by analyzing the propagation mechanism of a weather shock on agricultural production at a monthly frequency for various crops in heterogeneous geographical and seasonal patterns. We find that the growing process of crops generates a time lag between the realization and economic loss of the weather. An increase in both temperature and precipitation leads to a decline in production for up to four consecutive months for any crop in our sample. Responses appear to vary both in magnitude and duration, depending on the crop, with negative effects primarily driven by abnormally warm temperatures rather than increased precipitation.

As highlighted in the agronomic literature (Hatfield and Prueger, 2015), crop yield responses to weather shocks are highly dependent on the stage of plant development. We consider this point in the fourth section and find that, for each type of crop, production is damaged by a weather shock during both the growing and harvested phases, but the former period exhibits a stronger and longer effect than the latter. This result highlights the importance of shock timing, confirming that weather anomalies arising in the early growth stage have more prejudicial repercussions. Finally, we build on local projections to create a novel index of weather-driven losses. We find that a representative weather-driven loss shock causes a 0.9% loss in agricultural output, leading to a 0.15% reduction in GDP.

Our findings have substantial policy implications. First, using our estimates can be informative for policymakers to anticipate the future scarcity of agricultural products that arises a few months after the realization of a weather shock. A government observing an adverse weather shock can import agricultural products from other regions and countries to mitigate its detrimental effects before the economic consequences of the weather materialize at the harvesting stage. By dampening local fluctuations, such policies could be beneficial at the macroeconomic level, particularly for central banks, which target price stability. Our findings are also useful from the perspective of global warming, by identifying crops and regions that are the most weather-sensitive. Adap-

tation to climate change implies diversifying the agricultural supply towards crops that are more resistant to drought or flooded and waterlogged conditions.

This study also opens avenues for future research on higher frequencies weather shocks. First, the analysis could be extended to investigate price responses to weather variations rather than quantities. Based on macroeconomic quarterly data, the literature finds that aggregate prices decline following temperature shocks (Faccia et al., 2021; Natoli, 2022). Based on more granular data exploiting the cross-section of regions and crops, the analysis could investigate whether the disinflation nature of the weather holds at the regional level. Second, future research could be devoted to understanding how farmers anticipate El Niño events. Local market prices and quantities could react differently when a weather shock is surprised or anticipated news. Finally, the analysis could also be extended to investigate how local weather shocks can spread to other regions through trade interlinkages. With that respect, accommodating the international trade gravity model seems a promising avenue for future research.

References

Acevedo, S., Mrkaic, M., Novta, N., Pugacheva, E. and Topalova, P. (2020). The effects of weather shocks on economic activity: what are the channels of impact? Journal of Macroeconomics 65: 103207. 5

Aragón, F. M., Oteiza, F. and Rud, J. P. (2021). Climate change and agriculture: Subsistence farmers' response to extreme heat. American Economic Journal: Economic Policy 13: 1–35, doi:10.1257/pol.20190316. 2, 12

Auerbach, A. and Gorodnichenko, Y. (2011). Fiscal multipliers in recession and expansion. doi:10.3386/w17447. 19, 20, 21

Auffhammer, M., Hsiang, S. M., Schlenker, W. and Sobel, A. (2013). Using weather data and climate model output in economic analyses of climate change. Review of Environmental Economics and Policy 7: 181–198, doi:10.1093/reep/ret016. 9

Barrios, S., Bertinelli, L. and Strobl, E. (2010). Trends in rainfall and economic growth in africa: A neglected cause of the african growth tragedy. Review of Economics and Statistics 92: 350–366, doi:10.1162/rest.2010.11212. 8

Blanc, E. and Schlenker, W. (2017). The use of panel models in assessments of climate impacts on agriculture. Review of Environmental Economics and Policy 11: 258–279, doi:10.1093/reep/rex016. 4

Buchhorn, M., Smets, B., Bertels, L., De Roo, B., Lesiv, M., Tsendbazar, N.-E., Herold, M. and Fritz, S. (2020). Copernicus global land service: Land cover 100m: collection 3: epoch 2019: Globe. Version V3. 0.1)[Data set] doi:10.5281/zenodo.3939050. ii, iii

Burke, M. and Emerick, K. (2016). Adaptation to climate change: Evidence from us agriculture. American Economic Journal: Economic Policy 8: 106–40, doi:10.1257/pol.20130025. 3, 5

Castellanos, E., Lemos, M., Astigarraga, L., Chacón, N., Cuvi, N., Huggel, C., Miranda, L., Vale, M. M., Ometto, J., Peri, P., Postigo, J., Ramajo, L., Roco, L. and Rusticucci, M. (2022). Central and south america. In Pörtner, H. O., Roberts, D. C., Tignor, M., Poloczanska, E. S., Mintenbeck, K., Alegría, A., Craig, M., Langsdorf, S., Löschke, S., Möller, V., Okem, A. and Rama, B. (eds), Climate Change 2022: Impacts, Adaptation and Vulnerability. Contribution of Working Group II to the Sixth Assessment Report of the Intergovernmental Panel on Climate Change. Cambridge, UK and New York, USA: Cambridge University Press, 1689–1816, doi:10.1017/9781009325844.014.1689. 2

Colacito, R., Hoffmann, B. and Phan, T. (2019). Temperature and growth: A panel analysis of the united states. Journal of Money, Credit and Banking 51: 313–368. 3, 4

Crost, B., Duquennois, C., Felter, J. H. and Rees, D. I. (2018). Climate change, agricultural production and civil conflict: Evidence from the philippines. Journal of Environmental Economics and Management 88: 379–395, doi:10.1016/j.jeem.2018.01.005. 18

Cui, X., Gafarov, B., Ghanem, D. and Kuffner, T. (2022). On model selection criteria for climate change impact studies. 3

D'Agostino, A. L. and Schlenker, W. (2016). Recent weather fluctuations and agricultural yields: implications for climate change. Agricultural Economics 47: 159–171, doi:10.1111/agec.12315. 3, 4, 7, 9

Dell, M., Jones, B. F. and Olken, B. A. (2012). Temperature shocks and economic growth: Evidence from the last half century. American Economic Journal: Macroeconomics 4: 66–95, doi:10.1257/mac.4.3.66. 4, 14

Deschênes, O. and Greenstone, M. (2007). The economic impacts of climate change: evidence from agricultural output and random fluctuations in weather. American economic review 97: 354–385, doi:10.1257/aer.97.1.354. 3, 4, 9

Faccia, D., Parker, M. and Stracca, L. (2021). Feeling the heat: extreme temperatures and price stability. 4, 25, 27

Funk, C., Peterson, P., Landsfeld, M., Pedreros, D., Verdin, J., Shukla, S., Husak, G., Rowland, J., Harrison, L., Hoell, A. et al. (2015). CHIRPS: Rainfall estimates from rain gauge and satellite observations. doi:10.15780/G2RP4Q. 8

Gallic, E. and Vermandel, G. (2020). Weather shocks. European Economic Review 124: 103409, doi:10.1016/j.euroecorev.2020.103409. 23, 24, 26

Hatfield, J. L. and Prueger, J. H. (2015). Temperature extremes: Effect on plant growth and development. Weather and climate extremes 10: 4–10, doi:10.1016/j.wace.2015.08.001. 21, 26

Huerta, A., Aybar, C. and Lavado-Casimiro, W. (2018). PISCO temperatura v.1.1. Tech. rep., SENAMHI - DHI, Lima-Perú. 8

Iizumi, T. and Ramankutty, N. (2015). How do weather and climate influence cropping area and intensity? Global Food Security 4: 46–50, doi:10.1016/j.gfs.2014.11.003. 2

Jagnani, M., Barrett, C. B., Liu, Y. and You, L. (2020). Within-season producer response to warmer temperatures: Defensive investments by kenyan farmers. The Economic Journal 131: 392–419, doi:10.1093/ej/ueaa063. 3

Jordà, Ò. (2005). Estimation and inference of impulse responses by local projections. American economic review 95: 161–182, doi:10.1257/0002828053828518. 3, 16

Kolstad, C. D. and Moore, F. C. (2020). Estimating the economic impacts of climate change using weather observations. Review of Environmental Economics and Policy 14: 1–24, doi:10.1093/reep/rez024. 4, 5

Lesk, C., Rowhani, P. and Ramankutty, N. (2016). Influence of extreme weather disasters on global crop production. Nature 529: 84–87, doi:10.1038/nature16467. 3, 4

Letta, M., Montalbano, P. and Pierre, G. (2022). Weather shocks, traders' expectations, and food prices. American Journal of Agricultural Economics 104: 1100–1119, doi:10.1111/ajae.12258. 19

Massetti, E., Mendelsohn, R. and Chonabayashi, S. (2016). How well do degree days over the growing season capture the effect of climate on farmland values? Energy Economics 60: 144–150, doi:10.1016/j.eneco.2016.09.004. 19

Mendelsohn, R. (2009). The impact of climate change on agriculture in developing countries. Journal of Natural Resources Policy Research 1: 5–19, doi:10.1080/19390450802495882. 2

Mendelsohn, R., Nordhaus, W. D. and Shaw, D. (1994). The impact of global warming on agriculture: a ricardian analysis. The American economic review : 753–771. 4

Natoli, F. (2022). Temperature surprise shocks. doi:10.2139/ssrn.4160944. 5, 23, 25, 26, 27

Ortiz-Bobea, A., Ault, T. R., Carrillo, C. M., Chambers, R. G. and Lobell, D. B. (2021). Anthropogenic climate change has slowed global agricultural productivity growth. Nature Climate Change 11: 306–312, doi:10.1038/s41558-021-01000-1. 4

Ortiz-Bobea, A. and Just, R. E. (2012). Modeling the structure of adaptation in climate change impact assessment. American Journal of Agricultural Economics 95: 244–251, doi:10.1093/ajae/aas035. 7

Ortiz-Bobea, A., Wang, H., Carrillo, C. M. and Ault, T. R. (2019). Unpacking the climatic drivers of US agricultural yields. Environmental Research Letters 14: 064003, doi:10.1088/1748-9326/ab1e75. 7

Parry, M., Canziani, O., Palutikof, J., Linden, P. van der and Hanson, C. (2007). Fourth as-

sessment report: Climate change 2007: The ar4 synthesis report. Geneva: IPCC. URL http://www. ipcc. ch/ipccreports/ar4-wg1. htm . 2, 9

Powell, J. and Reinhard, S. (2016). Measuring the effects of extreme weather events on yields. Weather and Climate Extremes 12: 69–79, doi:10.1016/j.wace.2016.02.003. 7

Schlenker, W. and Roberts, M. J. (2009). Nonlinear temperature effects indicate severe damages to us crop yields under climate change. Proceedings of the National Academy of sciences 106: 15594–15598, doi:10.1073/pnas.0906865106. 4, 7

Schmitt, J., Offermann, F., Söder, M., Frühauf, C. and Finger, R. (2022). Extreme weather events cause significant crop yield losses at the farm level in german agriculture. Food Policy 112: 102359, doi:10.1016/j.foodpol.2022.102359. 7

Skees, J. R., Hartell, J. and Murphy, A. G. (2007). Using index-based risk transfer products to facilitate micro lending in peru and vietnam. American Journal of Agricultural Economics 89: 1255–1261, doi:10.1111/j.1467-8276.2007.01093.x. 18

Stock, J. H. and Watson, M. W. (2001). Vector autoregressions. Journal of Economic Perspectives 15: 101–115, doi:10.1257/jep.15.4.101. 24

Welch, J. R., Vincent, J. R., Auffhammer, M., Moya, P. F., Dobermann, A. and Dawe, D. (2010). Rice yields in tropical/subtropical asia exhibit large but opposing sensitivities to minimum and maximum temperatures. Proceedings of the National Academy of Sciences 107: 14562–14567, doi:10.1073/pnas.1001222107. 7, 19

Internet Appendix

(not for publication)

A Replication Codes

All the codes used to produce this article are available online.[24] We provide an ebook (https://egallic.fr/Recherche/weather-peru) that explains, step by step, how to reproduce the results, using R software. The scripts described in the notebook are also provided. They are divided into three parts:

1. Preparing the data
2. Replication of the estimations
3. Robustness checks.

B Definition of Weather-Adjusted Agricultural Losses

The weather component of agricultural losses, W_t (see Equation 11), is defined using a variable we denoted y_t^{ω} and termed "weather-adjusted agricultural production" (see Equation 11) following a five steps procedure. To calculate the weather component of agricultural losses, we follow a 5-step procedure.

Step 1: Estimating Weather Shock Contributions

In the first step, the contribution of weather shocks to a given crop (c) and time horizon (h) in each time period (t) is estimated. The weather shock contribution ($\Gamma_{c,i,t,h}$) is determined by considering the temperature ($T_{i,t}$) and precipitation ($P_{i,t}$), along with their respective coefficients ($\beta_{c,h}^T$ and $\beta_{c,h}^P$). This contribution is calculated as follows:

$$\Gamma_{c,i,t,h} = \beta_{c,h}^T T_{i,t-h} + \beta_{c,h}^P P_{i,t-h}. \tag{B.1}$$

Step 2: Calculating Quantity Weights

In the second step, we compute the quantity weights used in the third step. For each crop and date, these weights are defined by summing the monthly agricultural production over regions, expressed in monetary terms. The weights are calculated as follows:

$$\omega_{c,t} = \sum_i y_{c,t,i}^{\text{raw}} \times p_c, \tag{B.2}$$

where $y_{c,t,i}^{\text{raw}}$ represents the raw agricultural production in tons and p_c is the average selling price of crop c in our sample.

Step 3: Weather-Adjusted Agricultural Production

[24] https://www.dropbox.com/scl/fi/70r8h82sydgk2ubp9h6yv/Supplementary-materials.zip?rlkey=1iv2wy4g3y868d5h2nbb4l7e0&dl=0

Moving on to the third step, we calculate the weather-adjusted agricultural production ($y^{\omega}_{c,t}$) for each crop (c) at each date (t) is computed. This is achieved by summing the significant crop-specific contributions of weather ($\Gamma_{c,i,t,h}$) to agricultural production across regions as follows:

$$y^{\omega}_{c,t} = \sum_{h} \sum_{i} \frac{\mathbb{1}_{\text{signif}_{c,i,t,h}} \times \Gamma_{c,i,t,h} \times \omega_{c,t}}{\text{card}(I_{c,t})},$$

where card($I_{c,t}$) is the number of regions that produce crop c at time t, and the characteristic function $\mathbb{1}_{\text{signif}_{c,it,h}}$ equals 1 when the contribution is significantly different from 0 (based on the 95% confidence intervals of the coefficients $\beta^{T}_{c,h}$ and $\beta^{P}_{c,h}$), and 0 otherwise.

Step 4: Aggregating Crop-Specific Production

In the fourth step, crop-specific weather-adjusted agricultural production is aggregated at the national level, considering the quantity weights ($\omega_{c,t}$):

$$y^{\omega}_{t} = \frac{\sum_{c} y^{\omega}_{c,t}}{\sum_{c} \omega_{c,t}}, \tag{B.3}$$

where $\omega_{c,t}$ are the quantity weights computed in the second step.

Step 5: Expressing Weather-Adjusted Production as a Deviation

Finally, in the fifth step, the national weather-adjusted production is expressed as a loss or deviation from its trend. The trend is obtained using an HP filter:

$$WCAL_t = -100 \times (y^{\omega}_{t} - \overline{y^{\omega}_{t}}). \tag{B.4}$$

A negative sign is applied to ensure that the positive values of $WCLA_t$ correspond to losses rather than gains. Intuitively, W_t measures the percentage loss of agricultural value-added from weather shocks.

C Data

Table C.1 reports the total harvested area of Peru's main crops and their share of total annual production between 2001 and 2015. The surface area figures on which the article is based, i.e., those from the files of the Ministry of Agriculture of Peru (MINAGRI), are very close to those reported by the FAO. Those pertaining to the relative share of each crop are higher in the Ministry data. The crops included in the analyses carried out in the article represent almost two-thirds of production.

The map in Figure 2 shows the percentage of agricultural land for each cell corresponding to the weather data grid. These percentages are calculated from the Land Cover map data (Buchhorn et al., 2020). It can be noted that agricultural land is mainly located in the coastal regions and highlands, as shown in Figure C.1 and Figure C.2.

Table C.1. Main agricultural cultures in Peru

Product	FAO data		MINAGRI data	
	Total surface	Share	Total surface	Share (%)
Maize	7,349,640	16,4	4,227,147	14.7
Starchy corn			2,948,963	10.3
Rice, paddy	5,359,251	12.0	5,320,330	18.5
Coffee, green	4,999,410	11.1	-	-
Potatoes	4,213,436	9.4	4,151,734	14.5
Barley	2,253,611	5.0	2,233,429	7.8
Plantains and others	2,227,709	5.0	-	-
Wheat	2,158,122	4.8	2,102,246	7.3
Cassava	1,425,493	3.2	1,418,054	4.9
Sugar cane	1,112,131	2.5	1,032,231	3.6
Beans, dry	1,104,473	2.5	686,788	2.4

Notes: The products in bold are those studied in this study. The total surfaces correspond to the sum of national harvested surfaces, from 2001 to 2015, in hectares. Maize corresponds to Dent corn in the MINAGRI data. No distinction is made between Dent corn and Starchy corn in FAO data.
Source: FAO and MINAGRI. Author's estimate.

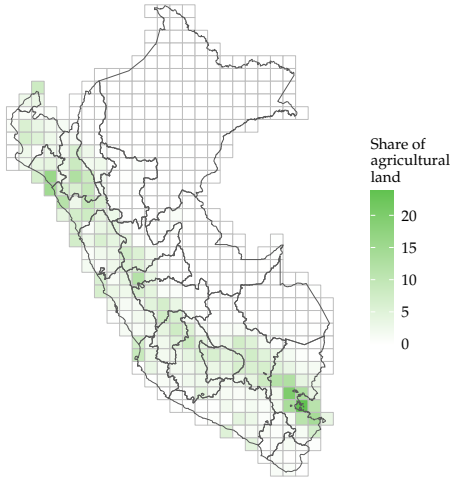

Notes: 2015 data, 100m resolution.
Source: Author's estimate using data from Buchhorn et al. (2020).

Figure C.1. Share of agricultural area in the cell, for each cell of the grid

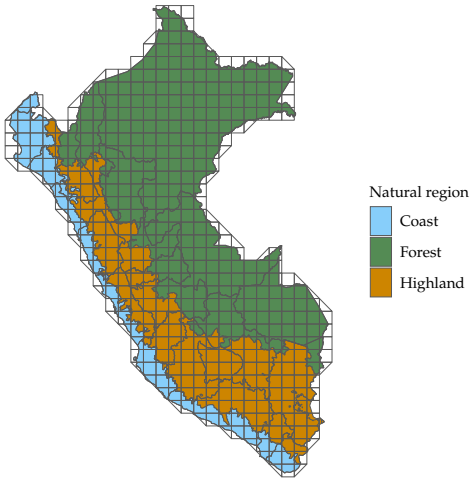

Source: Geo GPS Peru.

Figure C.2. Natural regions in Peru